

## Article

# Extractive Spectrophotometric Determination and Theoretical Investigations of Two New Vanadium(V) Complexes

 Kiril B. Gavazov <sup>1,\*</sup> , Petya V. Racheva <sup>1</sup> , Antoaneta D. Saravanska <sup>1</sup>, Galya K. Toncheva <sup>2</sup> and Vasil B. Delchev <sup>2</sup>
<sup>1</sup> Department of Chemical Sciences, Faculty of Pharmacy, Medical University of Plovdiv, 120 Buxton Bros Str., 4004 Plovdiv, Bulgaria

<sup>2</sup> Faculty of Chemistry, University of Plovdiv 'Paisii Hilendarskii', 24 Tsar Assen Str., 4000 Plovdiv, Bulgaria; vdelchev@uni-plovdiv.net (V.B.D.)

\* Correspondence: kiril.gavazov@mu-plovdiv.bg

**Abstract:** Two new vanadium (V) complexes involving 6-hexyl-4-(2-thiazolylazo)resorcinol (HTAR) and tetrazolium cation were studied. The following commercially available tetrazolium salts were used as the cation source: tetrazolium red (2,3,5-triphenyltetrazol-2-ium;chloride, TTC) and neotetrazolium chloride (2-[4-[4-(3,5-diphenyltetrazol-2-ium-2-yl)phenyl]phenyl]-3,5-diphenyltetrazol-2-ium;dichloride, NTC). The cations (abbreviated as TT<sup>+</sup> and NTC<sup>+</sup>) impart high hydrophobicity to the ternary complexes, allowing vanadium to be easily extracted and preconcentrated in one step. The complexes have different stoichiometry. The V(V)–HTAR–TTC complex dimerizes in the organic phase (chloroform) and can be represented by the formula [(TT<sup>+</sup>)[VO<sub>2</sub>(HTAR)]<sub>2</sub>. The other complex is monomeric (NTC<sup>+</sup>)[VO<sub>2</sub>(HTAR)]. The cation has a +1 charge because one of the two chloride ions remains undissociated: NTC<sup>+</sup> = (NT<sup>2+</sup>Cl<sup>-</sup>)<sup>+</sup>. The ground-state equilibrium geometries of the constituent cations and final complexes were optimized at the B3LYP and HF levels of theory. The dimer [(TT<sup>+</sup>)[VO<sub>2</sub>(HTAR)]<sub>2</sub> is more suitable for practical applications due to its better extraction characteristics and wider pH interval of formation and extraction. It was used for cheap and reliable extraction–spectrophotometric determination of V(V) traces in real samples. The absorption maximum, molar absorptivity coefficient, limit of detection, and linear working range were 549 nm, 5.2 × 10<sup>4</sup> L mol<sup>-1</sup> cm<sup>-1</sup>, 4.6 ng mL<sup>-1</sup>, and 0.015–2.0 μg mL<sup>-1</sup>, respectively.

**Keywords:** vanadium; 6-hexyl-4-(2-thiazolylazo)resorcinol; tetrazolium; liquid–liquid extraction; spectrophotometric determination; HF and B3LYP calculations



**Citation:** Gavazov, K.B.; Racheva, P.V.; Saravanska, A.D.; Toncheva, G.K.; Delchev, V.B. Extractive Spectrophotometric Determination and Theoretical Investigations of Two New Vanadium(V) Complexes.

*Molecules* **2023**, *28*, 6723.

<https://doi.org/10.3390/molecules28186723>

Academic Editor: Mannar R. Maurya

Received: 26 August 2023

Revised: 18 September 2023

Accepted: 19 September 2023

Published: 20 September 2023



**Copyright:** © 2023 by the authors. Licensee MDPI, Basel, Switzerland. This article is an open access article distributed under the terms and conditions of the Creative Commons Attribution (CC BY) license (<https://creativecommons.org/licenses/by/4.0/>).

## 1. Introduction

Vanadium can be classified as a dispersed trace element with an average content in the upper continental crust of 97 mg kg<sup>-1</sup> [1]. It enters the biosphere through natural phenomena (mechanical and chemical rock weathering, volcanism, forest fires, and aeolian processes) and human activity. The main sources of anthropogenic vanadium are ore mining and processing, fossil fuel combustion, agricultural chemicalization, and the production of glass, ceramics, pigments, rubber, redox batteries, plastics, and sulfuric acid [2–7]. Recently, its anthropogenic enrichment factors (AEFs) have increased: vanadium ranks first among the trace elements in the atmosphere and fourth among the trace elements in the world's rivers [2,5,8]. The problem is global [5] and should not be underestimated, as the most common anthropogenic vanadium form—V(V)—is almost as toxic as mercury, arsenic, lead, and cadmium [9]. This form resembles phosphorous (V) in chemical behavior [10] and can interfere with important biochemical processes by inhibiting the activity of key enzymes such as phosphatases and kinases [11,12].

Numerous methods based on coordination compounds have been used to determine V(V). Spectrophotometric methods are simple, cheap, and convenient [13–15]. They are often coupled with preconcentration techniques, which can greatly increase their range of

application [14–21]. In a previous paper, we described the application of the V(V)—6-hexyl-4-(2-thiazolylazo)resorcinol (HTAR) anionic chelate  $[\text{VO}_2(\text{HTAR})]^-$  [22] for the liquid–liquid extraction (LLE)–spectrophotometric determination of hydroxyzine hydrochloride in pharmaceuticals [23]. In the present paper, we set three goals:

1. To study the LLE of the V(V)–HTAR species in the presence of tetrazolium salt;
2. To find the ground-state equilibrium geometries of the extracted species using quantum chemical calculations at the B3LYP and HF levels of theory;
3. To develop a competitive LLE–spectrophotometric method for determining V(V) in real samples.

Tetrazolium salts (TSs) are an important class of compounds with versatile uses in chemistry, biology, and physics [24–31]. Two different TSs were used in this study: 2,3,5-triphenyltetrazol-2-ium;chloride (tetrazolium red, TTC) and 2-[4-[4-(3,5-diphenyltetrazol-2-ium-2-yl)phenyl]phenyl]phenyl]-3,5-diphenyltetrazol-2-ium;dichloride (neotetrazolium chloride, NTC) (Figure 1). They have found applications both as leuco dyes [24] and cationic-type ion-association reagents [25]. The association ability of their cations is governed by various factors such as molecular weight, number of tetrazolium rings, and nature of substituents in these rings [25,32,33]. Here, we concentrate on their application as ion-association reagents with special emphasis on the structure and extractability of the resulting complexes.

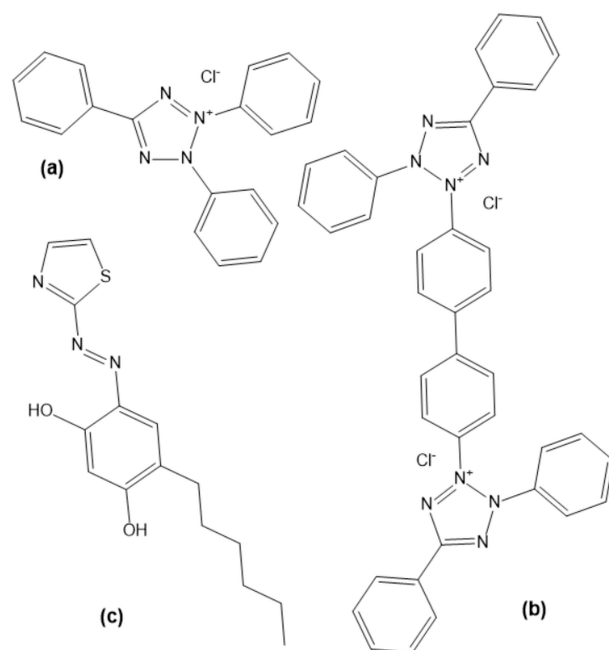


**Figure 1.** Structural formulae of the reagents TTC (a), NTC (b), and HTAR (c).

## 2. Results and Discussion

### 2.1. Absorption Spectra

The spectra of the extracted species are shown in Figure 2. The absorbance of the two complexes (1 and 2) at their absorption maxima ( $\lambda_{\text{max}}$ ) is practically the same. However, there is a small difference in the position of these maxima:  $\lambda_{\text{max}}$  (1) = 549 nm and  $\lambda_{\text{max}}$  (2) = 556 nm. The spectral band of the V(V)–HTAR–TTC complex (1) is slightly broader, which may be due to the aggregation of the extracted species [34].

The absorbance of the blank samples (1' and 2') at the absorption maxima of the corresponding complexes is low. Although the concentrations of the reagents under the optimal extraction conditions (see below) are higher for the HTAR–TTC system, the absorbance of the blank is lower. This is a prerequisite for achieving better repeatability with this TS.

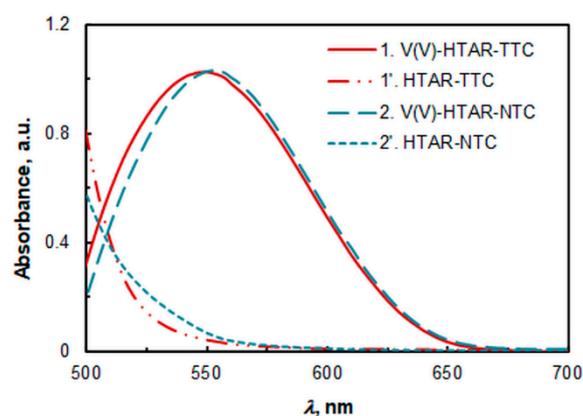


**Figure 2.** Absorption spectra of the V(V)-HTAR-TTC complex (1) and V(V)-HTAR-NTC complex (2) against corresponding blanks (1' and 2'). The spectra of the blanks (1' and 2') are recorded against chloroform.  $c_{V(V)} = 2 \times 10^{-5} \text{ mol L}^{-1}$ ,  $c_{HTAR} = 8 \times 10^{-5} \text{ mol L}^{-1}$  (1, 1') or  $4 \times 10^{-5} \text{ mol L}^{-1}$  (2, 2'),  $c_{TTC} = 2.4 \times 10^{-4} \text{ mol L}^{-1}$ ,  $c_{NTC} = 1.4 \times 10^{-4} \text{ mol L}^{-1}$ , and pH 5.0 (ammonium acetate buffer).

### 2.2. Effect of pH and the Amount of Buffer

The effect of pH was studied using a series of ammonium acetate buffer solutions with a known pH (Figure 3). The V(V)-HTAR-TTC complex is maximally extracted in a pH range of 3.9–5.0. The maximum extraction range of the V(V)-HTAR-NTC complex is shorter: 4.4–5.0. In this range, the absorbance of both complexes is the same.

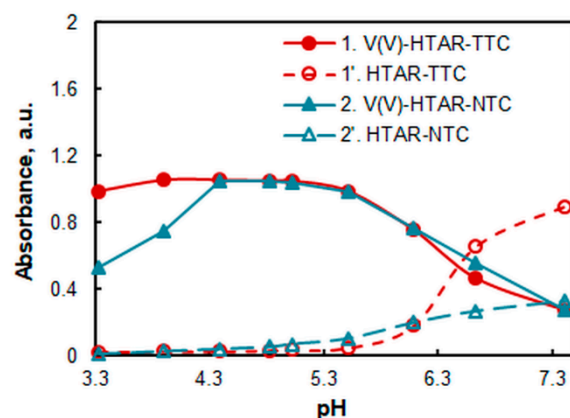


**Figure 3.** Absorbance of the complexes (1, 2) and blanks (1', 2') in chloroform vs. pH of aqueous phase.  $c_{V(V)} = 2 \times 10^{-5} \text{ mol L}^{-1}$ ,  $c_{HTAR} = 8 \times 10^{-5} \text{ mol L}^{-1}$  (1, 1') or  $4 \times 10^{-5} \text{ mol L}^{-1}$  (2, 2'),  $c_{TTC} = 2.4 \times 10^{-4} \text{ mol L}^{-1}$ ,  $c_{NTC} = 1.4 \times 10^{-4} \text{ mol L}^{-1}$ ,  $\lambda = 549 \text{ nm}$  (1, 1'), or  $556 \text{ nm}$  (2, 2').

To elucidate the effect of the amount of buffer, a series of experiments were carried out at pH 4.7 (one of the two pH values for which the buffering capacity is maximal [35]). It was found that there was no difference in absorbance in the presence of 1, 2, or 3 mL of the buffer solution. For reasons of economy, all subsequent experiments were performed with 1 mL of the buffer.

### 2.3. Effect of Extraction Time

The effect of extraction time is shown in Figure 4. Two minutes are needed to reach extraction equilibrium in the V(V)-HTAR-TTC system. Equilibrium in the other system is established a little slower (2.5 min). Since the shaking rate is a parameter that is difficult to control and depends on the experimenter, in order to avoid random and systematic errors, it is recommended that the extraction time be extended to 2.5 min and 3.0 min, respectively.

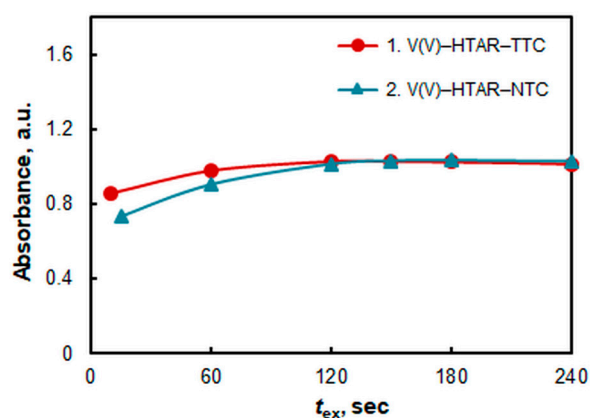


**Figure 4.** The effect of extraction time ( $t_{ex}$ ).  $c_{V(V)} = 2 \times 10^{-5} \text{ mol L}^{-1}$ ,  $c_{HTAR} = 8 \times 10^{-5} \text{ mol L}^{-1}$  (1) or  $4 \times 10^{-5} \text{ mol L}^{-1}$  (2),  $c_{TTC} = 2.4 \times 10^{-4} \text{ mol L}^{-1}$ ,  $c_{NTC} = 1.4 \times 10^{-4} \text{ mol L}^{-1}$ , and  $\text{pH} = 4.7$ .

#### 2.4. Effect of HTAR and TS Concentrations

The effect of the HTAR and TS (TTC or NTC) concentrations is shown in Figures 5 and 6, respectively. Saturation is more easily reached in the V(V)-HTAR-NTC system. The optimal reagent concentrations for the two systems, among other optimized parameters, are shown in Table 1.

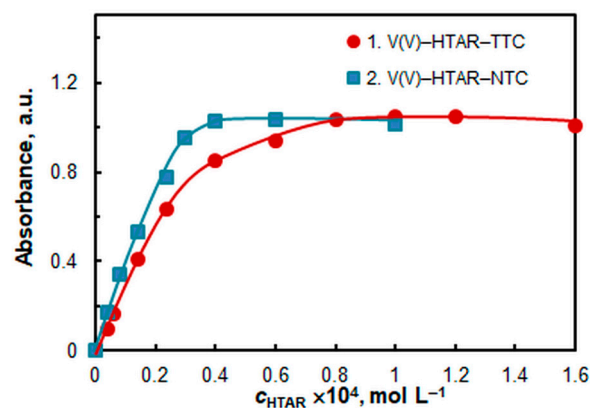


**Figure 5.** The effect of HTAR concentration.  $c_{V(V)} = 2 \times 10^{-5} \text{ mol L}^{-1}$ ,  $c_{TTC} = 6 \times 10^{-4} \text{ mol L}^{-1}$ ,  $c_{NTC} = 4 \times 10^{-4} \text{ mol L}^{-1}$ , and  $\text{pH} = 5.0$ .

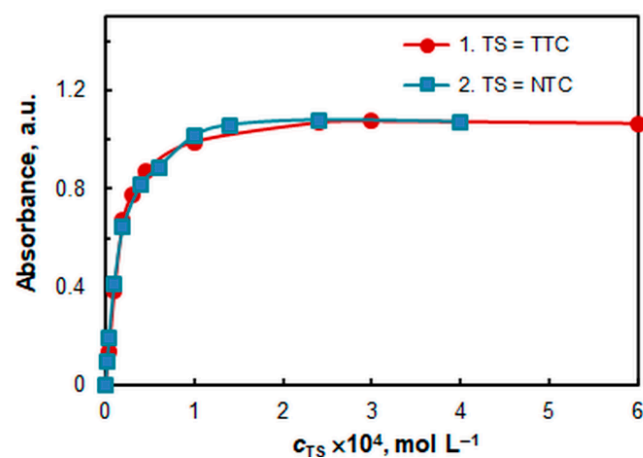


**Figure 6.** The effect of TS concentration. TS = TTC (1), TS = NTC (2).  $c_{V(V)} = 2 \times 10^{-5} \text{ mol L}^{-1}$ ,  $c_{HTAR} = 1 \times 10^{-4} \text{ mol L}^{-1}$  (1) or  $4 \times 10^{-5} \text{ mol L}^{-1}$  (2), and  $\text{pH} = 5.0$ .

**Table 1.** Optimum conditions <sup>a</sup>.

Extraction System	$\lambda_{\max}$ , nm	pH <sup>b</sup>	$c_{\text{HTAR}}$ , mol L <sup>-1</sup>	$c_{\text{TS}}$ , mol L <sup>-1</sup>	Extraction Time, min
V(V)–HTAR–TTC	549	4.7	$8 \times 10^{-5}$	$2.4 \times 10^{-4}$	2.5
V(V)–HTAR–NTC	556	4.7	$4 \times 10^{-5}$	$1.4 \times 10^{-4}$	3.0

<sup>a</sup> Optimization studies conducted at room temperature ( $22 \pm 1$  °C),  $V_{\text{aq}} = 10$  mL, and  $V_{\text{chloroform}} = 5$  mL.

<sup>b</sup> Ammonium acetate buffer (1 mL).

### 2.5. Stoichiometry, Formulas, and Equations

The small differences in the spectra (Figure 2) and optimal extraction conditions (Table 1) indicate possible differences in stoichiometry due to aggregation of the extracted species. Therefore, a variety of methods were used to elucidate the formulas of the complexes (Table 2), including those applicable to compounds of the type  $A_nB_m$  (where  $n = m > 1$ ) [36,37].

**Table 2.** Molar ratios in the ternary V(V)–HTAR–TS complexes obtained via different methods.

Molar Ratio	Mobile Equilibrium Method [36] <sup>a</sup>	Dilution Method [37] <sup>a</sup>	Job's Method [38,39] <sup>b</sup>	Asmus' Method [40] <sup>c</sup>	Bent–French Method [41] <sup>c</sup>
HTAR:V (TS = TTC)	2:2	–	–	1:1	1:1
HTAR:V (TS = NTC)	1:1	–	–	1:1	1:1
TTC:V	2:2	2:2	$n:n$ ( $n > 1$ )	1:1	1:1
NTC:V	1:1	–	–	1:1	1:1

<sup>a</sup> Methods applicable to complexes of the type  $A_2B_2$ . <sup>b</sup> A method capable of distinguishing  $A_1B_1$  complexes from  $A_nB_n$  ( $n > 1$ ) complexes. <sup>c</sup> Other methods with more limited capabilities.

Figures 7a and 8a present the results of determining the V(V):HTAR molar ratio in the ternary complexes via the mobile equilibrium method [36]. They show that the molar ratios in the two complexes are not the same: 2:2 (for the complex deriving from TTC) and 1:1 (for the complex deriving from NTC). This can be seen from the slopes ( $n$ ) of the obtained straight lines, which match well with the correct value of  $m$ .

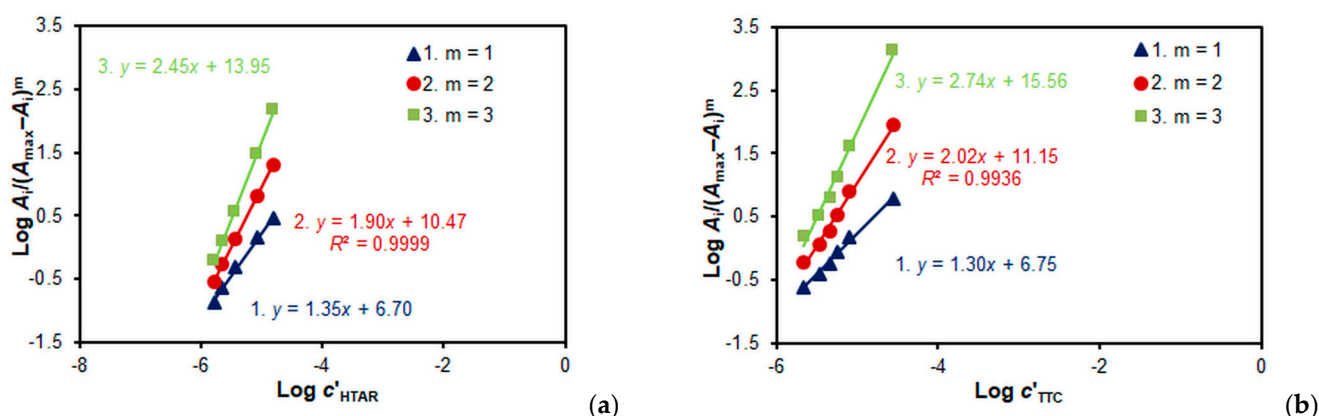


**Figure 7.** Determination of the HTAR:V(V) (a) and TTC:V(V) molar ratios in the V(V)–HTAR–TTC complex via the mobile equilibrium method.  $c_{V(V)} = 2 \times 10^{-5}$  mol L<sup>-1</sup>,  $c_{\text{TTC}} = 3 \times 10^{-4}$  mol L<sup>-1</sup> (a), and  $c_{\text{HTAR}} = 8 \times 10^{-5}$  mol L<sup>-1</sup> (b).

A similar conclusion is reached when studying the TS:V(V) molar ratio. When TS = TTC, the molar ratio is 2:2 (Figure 7b), and when TS = NTC, the molar ratio is 1:1 (Figure 8b).

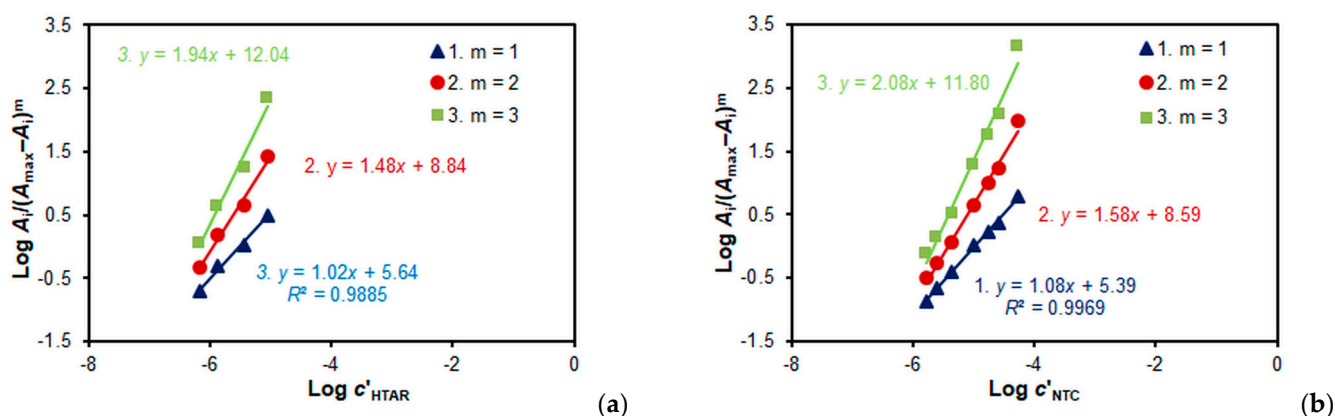


**Figure 8.** Determination of the HTAR:V(V) (a) and NTC:V(V) molar ratios in the V(V)–HTAR–NTC complex via the mobile equilibrium method.  $c_{\text{V(V)}} = 2 \times 10^{-5} \text{ mol L}^{-1}$ ,  $c_{\text{NTC}} = 4 \times 10^{-4} \text{ mol L}^{-1}$  (a), and  $c_{\text{HTAR}} = 4 \times 10^{-5} \text{ mol L}^{-1}$  (b).

An additional independent method [37] was used to confirm the stoichiometry in the TTC complex (Figure 9). As can be seen, a straight line is obtained for a complex of type  $A_2B_2$ .

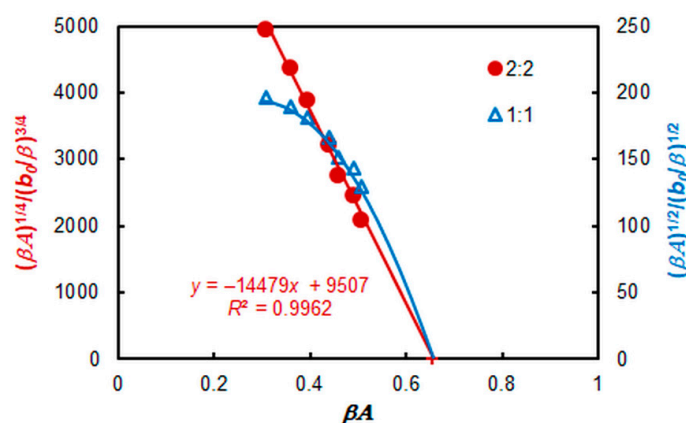


**Figure 9.** Determination of the TTC:V(V) molar ratio in the V(V)–HTAR–TTC complex via the dilution method.  $c_{\text{TTC}} = c_{\text{V(V)}}$ ,  $b_0 = 3 \times 10^{-5} \text{ mol L}^{-1}$ ,  $c_{\text{HTAR}} = 8 \times 10^{-5} \text{ mol L}^{-1}$ , and  $\text{pH} = 4.7$ .

It is known from the literature [39,42,43] that Job's method [38] can be used to distinguish 1:1-complexes from  $A_nB_n$  ( $n > 1$ ) complexes (e.g.,  $A_2B_2$ ,  $A_3B_3$ ,  $A_4B_4$ , etc.). The criterion for distinction is the presence or absence of concavities at the ends of the isomolar curve. Although such a distinction is not always reliable, it can be judged from Figure 10 that the NTC complex is most probably of the  $A_1B_1$  type (no concavities), and the TTC complex is of the  $A_nB_n$  type ( $n > 1$ ). If this conclusion is compared with the results presented above obtained via the mobile equilibrium method [36] and the dilution method [37], it can be deduced that  $n_{\text{TTC}}:n_{\text{V}} = 2:2$ .

The performed experiments give reason to assume that the complex obtained from TTC is an aggregate obtained in the organic phase via the dimerization of two 1:1:1 complexes represented by the formula  $(\text{TT}^+)[\text{VO}_2(\text{HTAR})]$ . Such dimerization was reported for similar extraction systems containing V(V) and 5-methyl-4-(2-thiazolylazo)resorcinol [44,45].

The complex of NTC is monomeric  $(\text{NTC}^+)[\text{VO}_2(\text{HTAR})]$ . The ditertazolium cation in it is most likely +1 charged:  $\text{NTC}^+ = [(\text{NT}^{2+})\text{Cl}^-]^+$ . This agrees with Tōei's concept of low charges ( $z = \pm 1$ ) of the ion-associable ions [32,46].

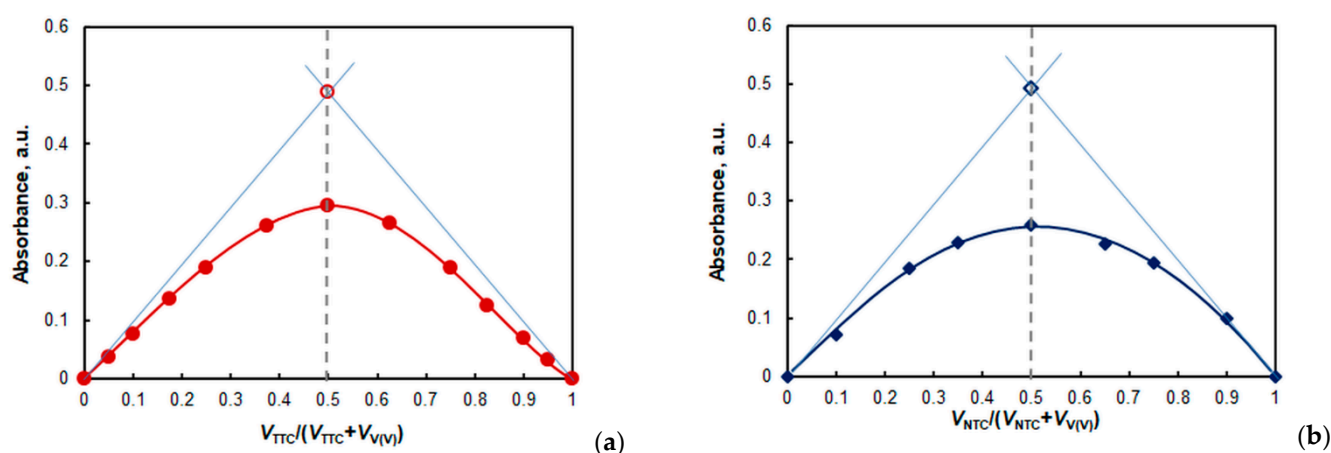
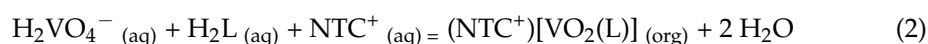
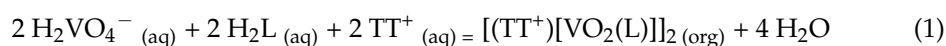


**Figure 10.** Job's method of continuous variations and Likussar–Boltz approach for the determination of  $K_{ex}$  in the V(V)—HTAR—TTC system (a) and V(V)—HTAR—NTC system (b).  $k = c_{V(V)} + c_{TS} = 4 \times 10^{-5} \text{ mol L}^{-1}$ ,  $c_{HTAR} = 8 \times 10^{-5} \text{ mol L}^{-1}$  (a) or  $4 \times 10^{-5} \text{ mol L}^{-1}$  (b), and  $\text{pH} = 4.7$ .

Equations of complex formation and extraction, based on information for the state of V(V) [13] and HTAR ( $\text{H}_2\text{L}$ ) [47,48] at the optimum pH value, are as follows:



## 2.6. Extraction Characteristics

Three independent methods were used to calculate the conditional extraction constant ( $K_{ex}$ ) characterizing Equation (1): the mobile equilibrium method [36] (Figure 7b, straight line 2), the dilution method [37] (Figure 9), and the Likussar–Boltz method [44,45,49] (Figure 10a).

The mobile equilibrium method (Figure 8b), Likussar–Boltz method (Figure 10b), Holme–Langmyhr method [50], and Harvey–Manning method [51] were used to determine the extraction constant for the NTC system (Equation (2)).

The obtained values, along with the values of distribution ratios ( $D$ ) and fractions extracted ( $E$ ), are given in Table 3.

**Table 3.** Calculated values of conditional extraction constants ( $K_{ex}$ ), distribution ratios ( $D$ ), and fractions extracted (% $E$ ).

Extraction System	Log $K_{ex}$					Log $D$	% $E$
	Mobile Equilibrium Method [36]	Dilution Method [37]	Likussar–Boltz Method [49]	Holme–Langmyhr Method [50]	Harvey–Manning Method [51]		
V(V)—HTAR—TTC	$15.2 \pm 0.4^a$	$15.8 \pm 0.1^c$	$15.2 \pm 0.1^d$ $15.1 \pm 0.1^e$	–	–	$1.53 \pm 0.08^h$	$97.1 \pm 0.5^h$
V(V)—HTAR—NTC	$5.0 \pm 0.1^b$	–	$5.1 \pm 0.1^f$	$5.0 \pm 0.1^g$	$5.0 \pm 0.1^h$	$0.94 \pm 0.14^i$	$90 \pm 3^i$

<sup>a</sup> Figure 7b; <sup>b</sup> Figure 8b; <sup>c</sup> Figure 9; <sup>d</sup> Figure 10a,  $k = 4 \times 10^{-5}$ ; <sup>e</sup>  $k = 1 \times 10^{-4}$ ; <sup>f</sup> Figure 10b; <sup>g</sup>  $N = 7$ ; <sup>h</sup>  $N = 3$ ; <sup>i</sup>  $N = 4$ .

## 2.7. Ground-State Equilibrium Geometries of the Cations

The optimized ground-state equilibrium geometries of the cations ( $\text{TT}^+$  and  $\text{NTC}^+$ ) are shown in Figure 11a,b. The five atoms in each of the tetrazolium rings are coplanar. The lengths of the N1–N5 and N2–N3 bonds in  $\text{TT}^+$  are equivalent (1.308 Å) and slightly shorter than the other bonds in this ring. The bond lengths between the atoms in the  $\text{NTC}^+$  rings are also close in length: N(1)–N(5) = 1.313 Å, N(2)–N(3) = 1.313 Å,

$N(1)-N(2) = 1.353 \text{ \AA}$ ,  $N(3)-C(4) = 1.352 \text{ \AA}$ , and  $N(5)-C(4) = 1.353 \text{ \AA}$  (left-hand ring), and  $N(24)-N(28) = 1.306 \text{ \AA}$ ,  $N(25)-N(26) = 1.305 \text{ \AA}$ ,  $N(24)-N(25) = 1.348 \text{ \AA}$ ,  $N(26)-C(27) = 1.351 \text{ \AA}$ , and  $N(28)-C(27) = 1.349 \text{ \AA}$  (right-hand ring). The lack of significant differences is consistent with the conclusion that the internal dimensions “are largely insensitive to the local environment” [30,52]. As seen in Figure 11b, the chloride ion is located near the right-hand tetrazolium ring (closest to N24). It is pinched by two hydrogen atoms (H(64) and H(61)) of the substituent groups.

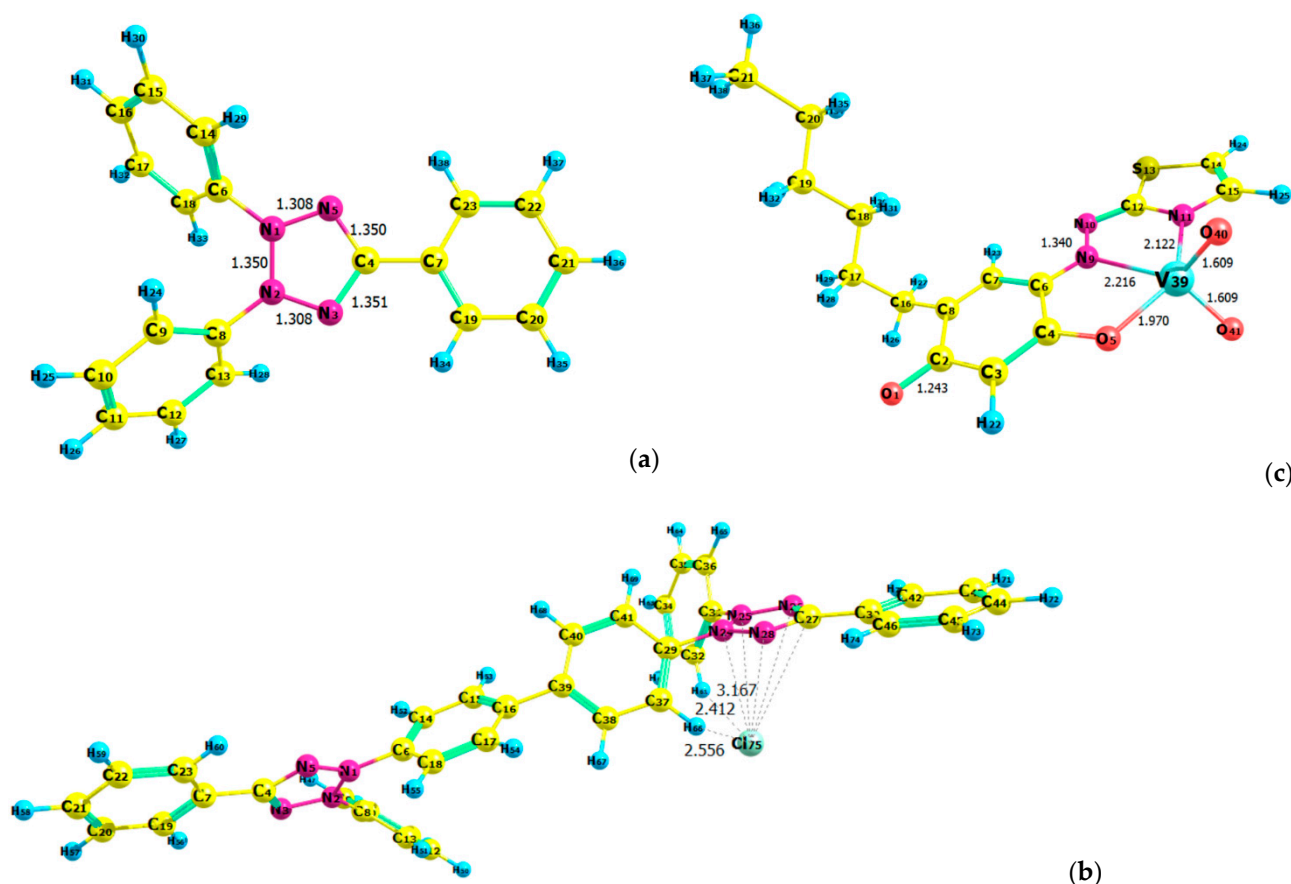


**Figure 11.** Optimized ground-state structures of the ions: TT<sup>+</sup> (B3LYP/6-311++G\*\*) (a), NTC<sup>+</sup> (B3LYP/6-31+G\*) (b), and [VO<sub>2</sub>(HTAR)]<sup>-</sup> (B3LYP/6-311++G\*\*) (c).

## 2.8. Ground-State Equilibrium Geometries of the Complexes

The next step was to correctly pair each of the two cationic structures (Figure 11a,b) with the anion [VO<sub>2</sub>(HTAR)]<sup>-</sup> optimized in a previous paper [23] (Figure 11c). Two different NTC<sup>+</sup>–[VO<sub>2</sub>(HTAR)]<sup>-</sup> structures were constructed and fully optimized at the HF/3–21G theoretical level (Figure 12a,b). Better stacking between the counterions was observed in Structure 1 (Figure 12a). Its energy is 15 kJ mol<sup>-1</sup> lower than that of Structure 2.

The structure of [(TT<sup>+</sup>)[VO<sub>2</sub>(HTAR)]]<sub>2</sub> was optimized in two steps. In the first step, the parent ions were assembled in two different ways, as shown in Figure 13a,b. In structure M1, the O(23) of the VO<sub>2</sub> group is located near the tetrazolium ring. In the more stable structure M2, both oxygen atoms from the VO<sub>2</sub> group are involved in additional interactions. Oxygen(24) is near the tetrazolium ring, and O(23) participates in a hydrogen bond C(50)–H(65)⋯O(23). This structure has 20 kJ mol<sup>-1</sup> lower energy.

Figure 14 shows structures of dimers obtained in the second step—pairing of monomers. The dimeric structure D1 (a) is derived from two structures, M1, the dimeric structure D2 (b) is derived from two structures, M2, and the dimeric structure D3 (c), is derived from one structure, M1, and one M2.

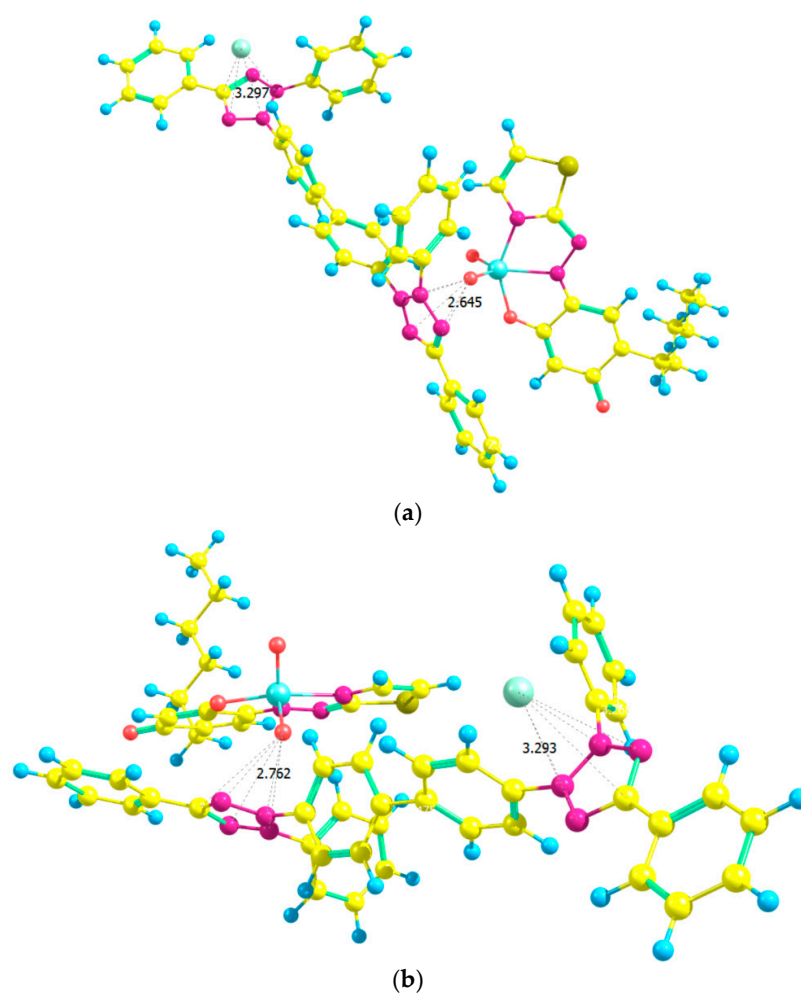


**Figure 12.** Optimized ground-state structures of the  $(\text{NTC}^+)[\text{VO}_2(\text{HTAR})]^-$  ion-association complex at the HF/3-21G theoretical level: (a) Structure 1,  $E_1 = -4706.2401$  a.u.,  $G_1 = -4705.3824$  a.u.,  $H_1 = -4705.2128$  a.u.; (b) Structure 2,  $E_2 = -4706.2345$  a.u.,  $G_2 = -4705.3779$  a.u.,  $H_2 = -4705.2073$  a.u.

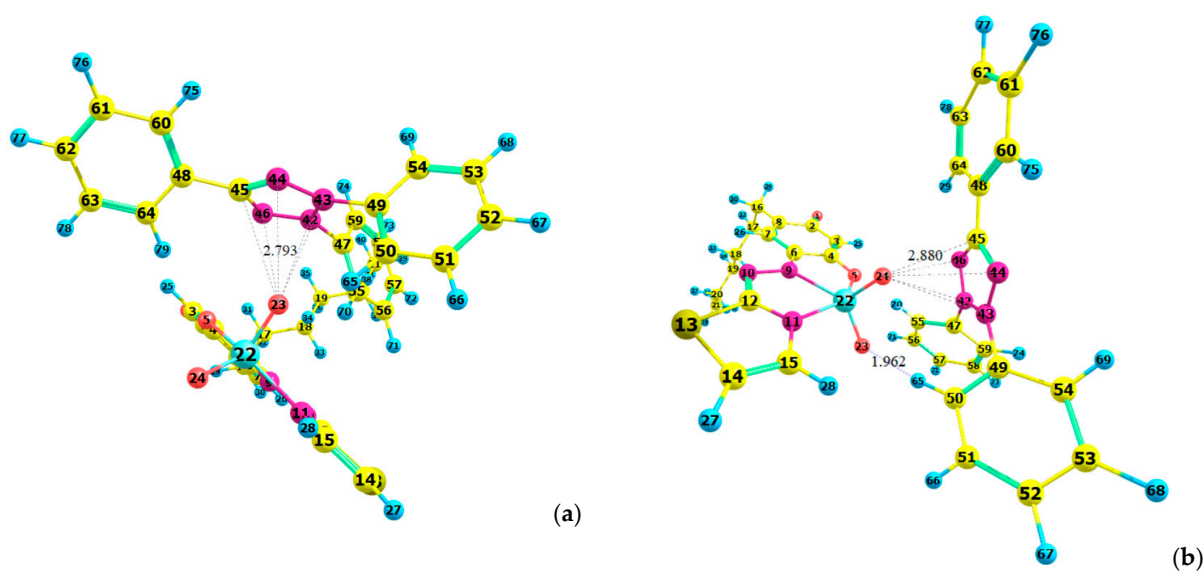


**Figure 13.** Optimized ground-state structures of the  $(\text{TT}^+)[\text{VO}_2(\text{HTAR})]$  monomer at the HF/3-21G theoretical level: (a) Structure M1,  $E_1 = -3309.4733$  a.u.,  $G_1 = -3308.8904$  a.u.,  $H_1 = -3308.7693$  a.u.; (b) Structure M2,  $E_2 = -3309.4656$  a.u.,  $G_2 = -3308.8823$  a.u.,  $H_2 = -3308.7619$  a.u.

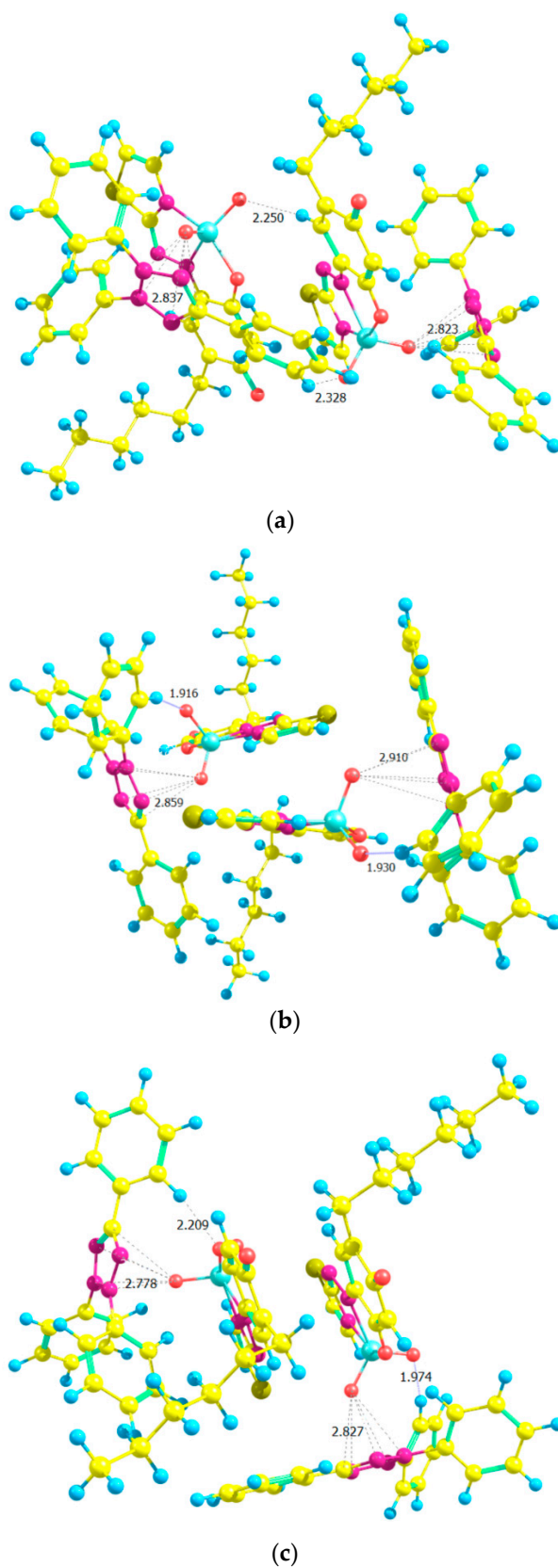


**Figure 14.** Optimized ground-state structures of the dimer  $[(TT^+)[VO_2(HTAR)]]_2$  at the HF/3-21G theoretical level: (a) Structure D1,  $E_1 = -6618.9481$  a.u.,  $G_1 = -6617.7571$  a.u.,  $H_1 = -6617.5383$  a.u.; (b) Structure D2,  $E_2 = -6618.9658$  a.u.,  $G_2 = -6617.7737$  a.u.,  $H_2 = -6617.5555$  a.u.; (c) Structure D3,  $E_3 = -6618.9454$  a.u.,  $G_3 = -6617.7531$  a.u.,  $H_3 = -6617.5359$  a.u.

The formation of D1 from two M1 structures is attended with a change of the Gibbs free energy of  $\Delta G^\circ_{298} = 20 \text{ kJ mol}^{-1}$  and heat effect of  $\Delta H^\circ_{298} = -38 \text{ kJ mol}^{-1}$ .

The structure D2 (Figure 14b) has  $46 \text{ kJ mol}^{-1}$  lower energy than the energy of D1. The change of  $\Delta G^\circ_{298}$  for the formation of the dimer from two M2 fragments is  $18 \text{ kJ mol}^{-1}$ , and the heat effect is  $\Delta H^\circ_{298} = -44 \text{ kJ mol}^{-1}$ .

The formation of the third dimer D3 is accompanied by  $\Delta G^\circ_{298} = 51 \text{ kJ mol}^{-1}$  and  $\Delta H^\circ_{298} = -12 \text{ kJ mol}^{-1}$ . The dimer complex has  $53 \text{ kJ mol}^{-1}$  higher energy than D2 and only  $7 \text{ kJ mol}^{-1}$  than D1. In other words, the energy analysis of the three V(V)–HTAR–TT complexes led to the following stability series:  $D2 > D1 > D3$ .

## 2.9. Analytical Characteristics and Application

The relationships between the measured absorbance and the V(V) concentration in the aqueous phase were investigated under optimal conditions (see Table 1). The linear regression equations and some associated parameters related to the application of these systems for the determination of V(V) are included in Table 4. Advantages of the TTC–HTAR system are a wider linear range, a lower LOD, a lower cost of TTC (in comparison to NTC), and the tolerance of higher amounts of side ions such as Al(III), Ba(II),  $\text{Br}^-$ , Ca(II),  $\text{Cl}^-$ , Cr(VI),  $\text{I}^-$ , Mo(VI),  $\text{NO}_3^-$ , and Re(VII) (Table 5). Advantages of the NTC–HTAR system are the lower reagents concentrations (Table 1) and higher tolerable levels of Zn(II), Cd(II), Hg(II), Mg(II), Pb(II),  $\text{F}^-$ , and  $\text{HPO}_4^{2-}$  (Table 5).

**Table 4.** Characteristics concerning the application of the two extraction–chromogenic systems for determining V(V).

Characteristics	HTAR–TTC System	HTAR–NTC System
Linear regression equation $y = ax + b$	$y = 1.020x + 0.0003$	$y = 1.018x - 0.005$
Correlation coefficient	0.9990 ( $N = 11$ )	0.9996 ( $N = 8$ )
Standard deviations of the slope ( $a$ ) and $y$ -intercept ( $b$ )	0.015 and 0.017	0.012 and 0.008
Linear range, $\mu\text{g mL}^{-1}$	0.015–2.0	0.023–1.1
Molar absorptivity coefficient ( $\epsilon$ ), $\text{L mol}^{-1} \text{ cm}^{-1}$	$5.2 \times 10^4$	$5.2 \times 10^4$
Sandell's sensitivity, $\text{ng cm}^{-2}$	0.98	0.98
Limit of detection (LOD) <sup>a</sup> , $\text{ng mL}^{-1}$	4.6	6.8
Limit of quantitation (LOQ) <sup>b</sup> , $\text{ng mL}^{-1}$	15	23

<sup>a</sup> Three times the standard deviation (SD) of the blank divided by the slope. <sup>b</sup> Ten times the SD of the blank divided by the slope.

**Table 5.** Effect of foreign ions on determining 5  $\mu\text{g}$  vanadium(V).

Foreign Ion (FI) Added	Added Salt Formula	HTAR–TTC System			HTAR–NTC System		
		FI:V(V) Mass Ratio	Amount of V(V) Found, $\mu\text{g}$	R, %	FI:V(V) Mass Ratio	Amount of V(V) Found, $\mu\text{g}$	R, %
Al(III)	$\text{Al}_2(\text{SO}_4)_3 \cdot 7\text{H}_2\text{O}$	1000	5.22	104	500	4.84	96.7
Ba(II)	$\text{Ba}(\text{NO}_3)_2$	2000 <sup>a</sup>	4.84	96.8	100	5.01	100
$\text{Br}^-$	NaBr	2000 <sup>a</sup>	4.93	98.6	1000	4.42	88.5
Ca(II)	$\text{Ca}(\text{NO}_3)_2 \cdot 4\text{H}_2\text{O}$	2000 <sup>a</sup>	5.01	100	250	4.93	98.5
Cd(II)	$3\text{CdSO}_4 \cdot 8\text{H}_2\text{O}$	5	5.13	103	500	4.91	98.2
		500	5.89	118	50	5.24	105
$\text{Cl}^-$	NaCl	10,000 <sup>a</sup>	5.02	100	500	4.97	99.4
Co(II)	$\text{CoSO}_4 \cdot 7\text{H}_2\text{O}$				250	4.81	96.3
Cr(III)	$\text{Cr}_2(\text{SO}_4)_3$	0.5	5.16	103	2000	4.58	91.6
Cr(VI)	$\text{KCrO}_4$	4	4.83	96.7	0.5	5.24	105
Cu(II)	$\text{CuSO}_4 \cdot 5\text{H}_2\text{O}$	500	4.87	97.4	5	5.19	104
		0.5	4.84	96.7	250	4.94	98.7
$\text{F}^-$	NaF	500	4.84	96.7	1	5.10	102
		1000	4.54	90.7	2000	5.02	100
					5000	4.40	88.0

Table 5. Cont.

Foreign Ion (FI) Added	Added Salt Formula	HTAR–TTC System			HTAR–NTC System		
		FI:V(V) Mass Ratio	Amount of V(V) Found, $\mu\text{g}$	R, %	FI:V(V) Mass Ratio	Amount of V(V) Found, $\mu\text{g}$	R, %
Fe(III)	Fe <sub>2</sub> (SO <sub>4</sub> ) <sub>3</sub>	0.5	5.28	106	0.5	5.42	108
					10 <sup>b</sup>	5.10	102
HPO <sub>4</sub> <sup>2-</sup>	Na <sub>2</sub> HPO <sub>4</sub>	2000	5.02	100	50 <sup>b</sup>	5.40	108
					2000 <sup>a</sup>	5.17	103
Hg(II)	Hg(NO <sub>3</sub> ) <sub>2</sub>	10	5.23	105	100	5.14	103
					1000	4.30	86.1
I <sup>-</sup>	KI	1000	4.84	96.9	10	4.30	86.1
					2000 <sup>a</sup>	5.06	101
Mg(II)	MgCl <sub>2</sub>	1000	4.73	94.7	2000 <sup>a</sup>	5.06	101
					100	5.04	101
Mn(II)	MnSO <sub>4</sub> ·H <sub>2</sub> O	500	5.32	106	500	5.23	105
					250	4.88	97.7
Mo(VI)	(NH <sub>4</sub> ) <sub>6</sub> Mo <sub>7</sub> O <sub>24</sub> ·4H <sub>2</sub> O	250	4.88	97.7	10	4.74	94.9
					2000 <sup>a</sup>	5.10	102
NO <sub>3</sub> <sup>-</sup>	NH <sub>4</sub> NO <sub>3</sub>	2000 <sup>a</sup>	5.10	102	1000	4.71	94.4
					0.5	5.15	103
Ni(II)	NiSO <sub>4</sub> ·6H <sub>2</sub> O	0.5	5.15	103	0.5	5.10	102
					10	4.81	96.3
Pb(II)	Pb(NO <sub>3</sub> ) <sub>2</sub>	10	4.81	96.3	20	4.99	99.8
					250	4.97	99.4
Re(VII)	NH <sub>4</sub> ReO <sub>4</sub>	500	4.71	94.1	5	4.97	99.4
					100	4.24	84.7
Tartrate <sup>2-</sup>	KNaC <sub>4</sub> H <sub>4</sub> O <sub>6</sub>	100	4.63	92.6	100	3.63	72.6
					1	7.29	146
V(IV)	VOSO <sub>4</sub> ·5H <sub>2</sub> O	1	7.29	146	1	7.10	142
					1	4.65	92.9
W(VI)	Na <sub>2</sub> WO <sub>4</sub> ·2H <sub>2</sub> O	1	4.65	92.9	1	4.91	98.3
					500	5.06	101
Zn(II)	ZnSO <sub>4</sub> ·7H <sub>2</sub> O	500	5.06	101	2000 <sup>a</sup>	4.83	96.7

<sup>a</sup> Higher FI:V(V) mass ratio not studied. <sup>b</sup> Masked by 10 mg F<sup>-</sup>.

The HTAR–TTC system was used to determine V(V) in real samples such as vanadium-depleted catalysts from sulfuric acid production and pharmaceuticals. The results of the catalyst analysis are shown in Table 6. They are statistically indistinguishable from those obtained via an alternative spectrophotometric method [53]. The results of V(V) determination in spiked pharmaceutical samples are displayed in Table 7. The recoveries were in the range of 97.2–105%, with relative standard deviations from 2.0% to 4.6%.

Table 6. Determination <sup>a</sup> of vanadium(V) in spent silica-supported catalysts.

Catalyst	Vanadium Found, %		RSD, %	
	HTAR–TTC Method	Alternative Method <sup>b</sup>	HTAR–TTC Method	Alternative Method <sup>b</sup>
Sample 1	2.96 ± 0.07	2.89 ± 0.12	2.4	4.2
Sample 2	2.42 ± 0.06	2.48 ± 0.11	2.5	4.4
Sample 3	2.99 ± 0.08	3.06 ± 0.11	2.7	3.6
Sample 4	1.95 ± 0.04	2.03 ± 0.09	2.1	4.4

<sup>a</sup> Four replicate analyses (mean ± standard deviation). <sup>b</sup> Ref. [53].

Table 7. Determination <sup>a</sup> of vanadium(V) in pharmaceutical samples.

Sample	V(V) Spike, ng mL <sup>-1</sup>	V(V) Found, ng mL <sup>-1</sup>	RSD, %	R, %
Sterimar nasal spray	0	Not detected	–	–
	25	24.3 ± 1.1	4.5	97.2
	50	51.7 ± 1.3	2.5	103
	75	73.9 ± 1.5	2.0	98.5
Marimer inhalation	0	Not detected	–	–
	25	26.3 ± 1.2	4.6	105
	50	49.4 ± 1.8	3.6	98.8
	75	75.2 ± 2.4	3.2	100
Solution for intravenous infusion	0	Not detected	–	–
	25	25.6 ± 0.8	3.1	102
	50	50.6 ± 1.3	2.6	101
	75	74.0 ± 2.3	3.1	98.6

<sup>a</sup> Three replicate analyses (mean ± standard deviation).

### 2.10. Comparison with Other Spectrophotometric Methods

Table 8 compares the performance of several spectrophotometric procedures for determining vanadium. The proposed HTAR–TTC procedure can be described as simple, cheap, fast, sensitive, and reliable. It does not require any special or expensive equipment and is easier to implement than DLLME-SFOD [54], UA-CPE [17,55], or MA-CPE [53]. It is faster than many procedures requiring prolonged extraction (10–20 min) [16,21,56], centrifugation + cooling (10 min) [54], sonification at elevated temperature + centrifugation + cooling (17–28 min) [17,55], incubation at elevated temperature + cooling (55–110 min) [53,57], or two-fold extraction [21]. The sensitivity is higher than that of most liquid–liquid extraction (LLE) procedures [16,19–21,58,59], and the amount of organic solvent used is less than that of some of them [20,21,44,58]. Reagents are commercially available, and there is no need for tedious syntheses as described in [21,56,58,60]. Finally, the procedure can be considered reliable as the optimal intervals are wide enough and none of the thoroughly investigated parameters is problematic.

**Table 8.** Comparison with other spectrophotometric procedures.

Reagent(s)	Preconcentration Technique	$\lambda_{\max}$ , nm	$\epsilon \times 10^{-4}$ , L mol <sup>-1</sup> cm <sup>-1</sup>	Linear Range, $\mu\text{g mL}^{-1}$	LOD, ng mL <sup>-1</sup>	Application	Ref.
APANOL	–	533	1.02	0.1–4.00	54	Rise and flour	[60]
BPHA	LLE	530	0.545	Up to 1.5	–	Water samples	[19]
CV + KI	–	588	1.27	0.1–10.2	675	Soil, biological, and pharmaceutical samples	[61]
DTP + Amines	LLE	615–620	2.8–3.0	0.05–16	–	Soils, oil, and oil products	[16]
EDTA + ST	UA-CPE	530	–	0.002–0.18	0.26	Vegetal oils and vinegar	[55]
HPMEPB	LLE	415	2.7	Up to 2.2	79.2	Synthetic and technical samples	[58]
MQ	LLE	400	0.2449	Up to 6.2	168	–	[20]
PCNPC4RAHA	LLE	495	0.554	0.137–9.36	8.89	Steels, environmental and biological samples	[21]
PG + ST	UA-CPE	533	–	0.002–0.5	0.58	Beverage samples	[17]
TA + CTAB	DLLME-SFOD	600	–	0.006–1	1.8	Fruit juice samples	[54]
TAN + H <sub>2</sub> O <sub>2</sub>	MA-CPE	607	8.84	Up to 0.76	1.4	Mineral water, pharmaceutical, and industrial samples	[53]
HTAR + NTC	LLE	556	5.2	0.023–1.1	6.8	–	This work
HTAR + TTC	LLE	549	5.2	0.015–2.0	4.6	Catalysts and pharmaceuticals	This work

Abbreviations: APANOL, 1-[(4-Antipylazo)]-2-naphthol; BPHA, *N*-benzoyl-*N*-phenylhydroxylamine; CTAB, cetyltrimethylammonium bromide; CV, crystal violet; DTP, 2,6-Dithiolphenol; DLLME-SFOD, dispersive liquid–liquid microextraction based on solidified floated organic drop; EDTA, ethylenediaminetetraacetic acid; HPMEPB, 3-Hydroxy-2-[3-(4-methoxyphenyl)-1-phenyl-4-pyrazolyl]-4-oxo-4*H*-1-benzopyran; LLE, liquid–liquid extraction; MA-CPE, microwave-assisted cloud point extraction; MQ, 2-Methyl-8-quinolinol; PCNPC4RAHA, *p*-Carboxy-*N*-phenyl-calix [4]resorcinarene-hydroxamic acid; PG, pyrogallol; ST, safranin T; TA, tannic acid; TAN, 1-(2-thiazolylazo)-2-naphthol; UA-CPE, ultrasound-assisted cloud point extraction.

## 3. Materials and Methods

### 3.1. Reagents and Chemicals

Reagents from Merck (Schnellendorf, Germany), Fluka (Buchs, Switzerland), and Loba Feinchemie (Fischamend, Austria) were used without additional purification as aqueous solutions. The standard solution of V(V) was prepared from NH<sub>4</sub>VO<sub>3</sub> (Merck, puriss. p. a.) at a concentration of  $2.0 \times 10^{-4}$  mol L<sup>-1</sup>. Solutions of TTC (Loba Feinchemie, p.a.) and NTC (Fluka, for microbiology) were stored in dark flasks;  $c_{\text{TTC}} = 3 \times 10^{-3}$  mol L<sup>-1</sup> and  $c_{\text{NTC}} = 2 \times 10^{-3}$  mol L<sup>-1</sup>. The azo dye HTAR (Merck) was dissolved in the presence of KOH [22,57,62];  $c_{\text{HTAR}} = 2 \times 10^{-3}$  mol L<sup>-1</sup>. A series of buffer solutions (pH 3.3–7.4) were made by mixing 2 mol L<sup>-1</sup> solutions of acetic acid and ammonia. Chloroform was purified by distillation and used repeatedly according to safety regulations. Distilled water was used in all experiments.

### 3.2. Instrumentation

An Ultrospec 3300 pro scanning spectrophotometer (Garforth, UK), equipped with 10 mm path-length quartz (or glass) cuvettes, was used during the work. The pH measurements were made with a WTW InoLab 7110 pH meter (Weilheim, Germany) with a glass electrode.

### 3.3. Samples

Pharmaceuticals were purchased from a local pharmacy: (i) Marimer inhalation (2.2% hypertonic seawater); (ii) Sterimar for nasal hygiene (a 100% natural, purified seawater-based nasal spray); and (iii) a solution of 0.9% NaCl for intravenous infusion. Aliquots of 5 mL of these solutions were subjected to the extraction procedure.

Samples of spent silica-supported catalysts (from the sulfuric acid production) were provided by KCM SA, Plovdiv (Bulgaria). They were ground in a mortar and prepared for analysis according to a known procedure [59]. Aliquots of 0.5 mL of the obtained solutions were used for the analysis.

### 3.4. Procedures for Optimization and Determination of Extraction Constants

The following solutions were mixed in a 125 mL separatory funnel: V(V), ammonium acetate buffer, HTAR, and TS (TTC or NTC). Water was added to a total volume of 10 mL. The volume of chloroform was 5 mL (in the optimization experiments) or 10 mL (in the determination of the extraction constant; Figures 7–10). After pouring the organic solvent, the funnel was stoppered and shaken for a fixed time. Part of the resulting chloroform extract was filtered through filter paper and transferred to the cuvette. Absorbance was measured against a simultaneously prepared blank containing no V(V).

### 3.5. Procedure for Determination of Distribution Ratios and Fractions Extracted

The liquid–liquid distribution ratios for each of the systems were calculated after considering the absorbance in single extraction ( $A_1$ ) and triple extraction ( $A_3$ ) experiments:  $D = A_1 / (A_3 - A_1)$ . The single extraction and the first step of the triple extraction were performed with 10 mL of chloroform under the optimal extraction conditions (Table 1). The organic layers were transferred into 25 mL volumetric flasks. The flask for the single extraction was brought to the mark with chloroform. The second and third steps of the triple extraction were carried out by adding 7 mL of chloroform to the aqueous phase of the previous step. The organic extracts were combined in the second 25 mL volumetric flask, and chloroform was added to the mark. Absorbances were measured against corresponding blanks.

The fractions extracted were calculated using the equation  $\%E = 100 \times D / (D + 1)$ .

### 3.6. Procedure for Determination of Vanadium(V) with HTAR and TTC

An aliquot of the analyzed solution (containing 0.015–2.0  $\mu\text{g mL}^{-1}$  of V) was transferred in a 125 mL separatory funnel. Solutions of the buffer (1 mL, pH 4.7), HTAR (0.4 mL,  $2 \times 10^{-3} \text{ mol L}^{-1}$ ), and TTC (0.8 mL,  $3 \times 10^{-3} \text{ mol L}^{-1}$ ) were added, and the sample was diluted with water until a total volume of 10 mL. Then, 5 mL of chloroform was added, and the mixture was shaken for 2.5 min. After the phase separation, a portion of the chloroform extract was poured into the cuvette, and the absorbance was measured at 549 nm against a blank. The unknown V(V) concentration was calculated from a calibration plot prepared using the same procedure.

### 3.7. Procedure for Determination of Vanadium(V) with HTAR and NTC

An aliquot of the analyzed solution (containing 0.023–1.1  $\mu\text{g mL}^{-1}$  of V) was transferred in a 125 mL separatory funnel. Solutions of the buffer (1 mL, pH 4.7), HTAR (0.2 mL,  $2 \times 10^{-3} \text{ mol L}^{-1}$ ), and NTC (0.7 mL,  $2 \times 10^{-3} \text{ mol L}^{-1}$ ) were added, and the sample was diluted with water until a total volume of 10 mL. Then, 5 mL of chloroform was added, and the mixture was shaken for 3.0 min. After the phase separation, a portion of the chloroform

extract was poured into the cuvette, and the absorbance was measured at 556 nm against a blank. The unknown V(V) concentration was calculated from a calibration plot prepared using the same procedure.

### 3.8. Theoretical

The ground-state equilibrium geometries of the cations,  $\text{TT}^+$  and  $\text{NTC}^+$ , were optimized at the B3LYP/6-311++G\*\* and B3LYP/6-31+G\* levels of theory, respectively. Each of these cations was then paired in different ways with the anionic complex  $[\text{VO}_2(\text{HTAR})]^-$  studied in a previous work [23] as described above.

The  $\text{NTC}^+$  and  $[\text{VO}_2(\text{HTAR})]^-$  counterions were assembled in two ways and optimized at the HF/3-21G level of theory. Furthermore, the thermodynamic characteristics of the obtained structures were calculated and compared.

The  $\text{TT}^+$  and  $[\text{VO}_2(\text{HTAR})]^-$  counterions were also assembled in two different ways and optimized at the HF/3-21G level of theory to obtain monomeric structures (M1 and M2) of the type  $(\text{TT}^+)[\text{VO}_2(\text{HTAR})]$ . These structures were combined into three dimers (M1–M1, M2–M2, and M1–M2). Optimization was performed at the HF/3-21G level of theory, and the stability of the obtained species was evaluated.

All calculations were performed for the gas phase using the GAUSSIAN 16 program package [63]. The ChemCraft program (<https://chemcraftprog.com> (accessed on 13 September 2023)) was used for the visualization of the computed results [64].

## 4. Conclusions

The complex formation of two new V(V) complexes has been studied. The differences between the extracted species have been highlighted. The behavior of the ditetrazolium salt NTC is interesting because of its participation in the final complex as a singly charged cation  $[(\text{NT})^{2+}\text{Cl}^-]^+$ . The  $\text{TT}^+$  complex, on the other hand, is notable for its dimeric structure, which gives it excellent extractability and good analytical characteristics. It has been applied to the analysis of real samples—pharmaceuticals and silica-supported catalysts.

**Author Contributions:** Conceptualization, K.B.G.; methodology, K.B.G., P.V.R. and V.B.D.; software, V.B.D. and K.B.G.; validation, K.B.G., P.V.R. and A.D.S.; formal analysis, K.B.G., P.V.R. and V.B.D.; investigation, P.V.R., A.D.S. and G.K.T.; resources, K.B.G., V.B.D. and G.K.T.; writing—original draft preparation, K.B.G.; writing—review and editing, V.B.D. and K.B.G.; visualization, K.B.G., G.K.T. and A.D.S.; supervision, K.B.G.; project administration, V.B.D.; funding acquisition, K.B.G. All authors have read and agreed to the published version of the manuscript.

**Funding:** This research was funded in part by the National Centre for High-performance and Distributed Computing through grant No D01-168/28.07.2022. The APC will be funded by the Medical University of Plovdiv.

**Institutional Review Board Statement:** Not applicable.

**Informed Consent Statement:** Not applicable.

**Data Availability Statement:** Not applicable.

**Acknowledgments:** We acknowledge the provided access to the e-infrastructure of the NCHDC, a part of the Bulgarian National Roadmap on RIs, with financial support by Grant No D01-168/28.07.2022.

**Conflicts of Interest:** The authors declare no conflict of interest.

**Sample Availability:** Not available.

## References

1. Rudnick, R.L.; Gao, S. *Treatise on Geochemistry*, 2nd ed.; Holland, H.D., Turekian, K.K., Eds.; Elsevier: Oxford, UK, 2014; Volume 4, pp. 1–51. [\[CrossRef\]](#)
2. Schlesinger, W.H.; Klein, E.M.; Vengosh, A. Global biogeochemical cycle of vanadium. *Proc. Natl. Acad. Sci. USA* **2017**, *114*, E11092–E11100. [\[CrossRef\]](#) [\[PubMed\]](#)
3. Roychoudhury, A. Vanadium uptake and toxicity in plants. *SF J. Agri. Crop Manag.* **2020**, *1*, 1010.
4. Hope, B.K. A dynamic model for the global cycling of anthropogenic vanadium. *Glob. Biogeochem. Cycles* **2008**, *22*, GB4021. [\[CrossRef\]](#)
5. Watt, J.A.; Burke, I.T.; Edwards, R.A.; Malcolm, H.M.; Mayes, W.M.; Olszewska, J.P.; Pan, G.; Graham, M.C.; Heal, K.V.; Rose, N.L.; et al. Vanadium: A re-emerging environmental hazard. *Environ. Sci. Technol.* **2018**, *52*, 11973–11974. [\[CrossRef\]](#) [\[PubMed\]](#)
6. Wlazłowska, E.; Grabarczyk, M. Adsorptive Stripping Voltammetry for Determination of Vanadium: A Review. *Materials* **2023**, *16*, 3646. [\[CrossRef\]](#)
7. Imtiaz, M.; Rizwan, M.S.; Xiong, S.; Li, H.; Ashraf, M.; Shahzad, S.M.; Shahzad, M.; Rizwan, M.; Tu, S. Vanadium, recent advancements and research prospects: A review. *Environ. Int.* **2015**, *80*, 79–88. [\[CrossRef\]](#)
8. Viers, J.; Dupré, B.; Gaillardet, J. Chemical composition of suspended sediments in World Rivers: New insights from a new database. *Sci. Total Environ.* **2009**, *407*, 853–868. [\[CrossRef\]](#)
9. Vasseghian, Y.; Sadeghi Rad, S.; Vilas-Boas, J.A.; Khataee, A. A global systematic review, meta-analysis, and risk assessment of the concentration of vanadium in drinking water resources. *Chemosphere* **2021**, *267*, 128904. [\[CrossRef\]](#)
10. Rayner-Canham, G. Periodic patterns: The Group (n) and Group (n + 10) linkage. *Found. Chem.* **2013**, *15*, 229–237. [\[CrossRef\]](#)
11. Rehder, D. The role of vanadium in biology. *Metallomics* **2015**, *7*, 730–742. [\[CrossRef\]](#)
12. Rehder, D. Vanadium in health issues. *ChemTexts* **2018**, *4*, 20. [\[CrossRef\]](#)
13. Taylor, M.J.C.; Staden, J.F. Spectrophotometric determination of vanadium(IV) and vanadium(V) in each other's presence. *Analyst* **1994**, *119*, 1263–1276. [\[CrossRef\]](#)
14. Pyrżyńska, K. Recent developments in spectrophotometric methods for determination of vanadium. *Microchim. Acta* **2005**, *149*, 159–164. [\[CrossRef\]](#)
15. He, W.-Y.; Wang, K.-P.; Yang, J.-Y. Spectrophotometric methods for determination of vanadium: A review. *Toxicol. Environ. Chem.* **2018**, *100*, 20–31. [\[CrossRef\]](#)
16. Kuliyeve, K.A.; Verdizade, N.A. Spectroscopic investigation complex formation of vanadium using 2,6-dithiolphenol and hydrofobamins. *Am. J. Chem.* **2015**, *5*, 10–18.
17. Temel, N.K.; Gürkan, R. Preconcentration and determination of trace vanadium(V) in beverages by combination of ultrasound assisted-cloud point extraction with spectrophotometry. *Acta Chim. Slov.* **2018**, *65*, 138–149. [\[CrossRef\]](#)
18. Stefanova, T.S.; Simitchiev, K.K.; Gavazov, K.B. Liquid-liquid extraction and cloud point extraction for spectrophotometric determination of vanadium using 4-(2-pyridylazo) resorcinol. *Chem. Pap.* **2015**, *69*, 495–503. [\[CrossRef\]](#)
19. Bychkova, O.A.; Zavadova, M.N.; Nikitina, T.G.; Nikonorov, V.V. Extraction-photometric determination of vanadium in natural waters. *J. Anal. Chem.* **2015**, *70*, 962–966. [\[CrossRef\]](#)
20. Singh, S.; Nivedita, A.; Parveen, R.; Rajesh, A.; Vikas, K. Molecular dynamics, biological study and extractive spectrophotometric determination of vanadium (V)-2-methyl-8-quinolinol complex. *Iran. J. Chem. Chem. Eng.* **2021**, *40*, 207–214. [\[CrossRef\]](#)
21. Pillai, S.G.; Dwivedi, A.H.; Patni, N. Liquid-liquid extraction and spectrophotometric determination of vanadium(V) with p-carboxy-n-phenyl-calix[4]resorcinarene-hydroxamic acid. *Procedia Eng.* **2013**, *51*, 347–354. [\[CrossRef\]](#)
22. Hristov, D.; Milcheva, N.; Gavazov, K. Extraction-chromogenic systems for vanadium(V) based on azo dyes and xylometazoline hydrochloride. *Acta Chim. Slov.* **2019**, *66*, 987–994. [\[CrossRef\]](#) [\[PubMed\]](#)
23. Kirova, G.K.; Velkova, Z.Y.; Delchev, V.B.; Gavazov, K.B. Vanadium-Containing Anionic Chelate for Spectrophotometric Determination of Hydroxyzine Hydrochloride in Pharmaceuticals. *Molecules* **2023**, *28*, 2484. [\[CrossRef\]](#) [\[PubMed\]](#)
24. Daniel, D.S. The chemistry of tetrazolium salts. In *Chemistry and Applications of Leuco Dyes*; Muthyala, R., Ed.; Kluwer Academic Publishers: New York, NY, USA, 2002; pp. 207–296. [\[CrossRef\]](#)
25. Gavazov, K.B.; Dimitrov, A.N.; Lekova, V.D. The use of tetrazolium salts in inorganic analysis. *Russ. Chem. Rev.* **2007**, *76*, 169–179. [\[CrossRef\]](#)
26. Creanga, D.; Nadejde, C. Molecular modelling and spectral investigation of some triphenyltetrazolium chloride derivatives. *Chem. Pap.* **2014**, *68*, 260–271. [\[CrossRef\]](#)
27. Voitekhovich, S.V.; Lesnyak, V.; Gaponik, N.; Eychmüller, A. Tetrazoles: Unique Capping Ligands and Precursors for Nanostructured Materials. *Small* **2015**, *11*, 5728–5739. [\[CrossRef\]](#)
28. Penev, K.I.; Wang, M.; Mequanint, K. Tetrazolium salt monomers for gel dosimetry I: Principles. *J. Phys. Conf. Ser.* **2017**, *847*, 012048. [\[CrossRef\]](#)
29. Li, X.; Deng, S.; Lin, T.; Xie, X.; Xu, X. Inhibition action of triazolyl blue tetrazolium bromide on cold rolled steel corrosion in three chlorinated acetic acids. *J. Mol. Liq.* **2019**, *274*, 77–89. [\[CrossRef\]](#)
30. Bakheit, A.H.; Ghabbour, H.A.; Hussain, H.; Al-Salahi, R.; Ali, E.A.; Mostafa, G.A.E. Synthesis and computational and X-ray structure of 2,3,5-triphenyl tetrazolium, 5-ethyl-5-phenylbarbituric acid salt. *Crystals* **2022**, *12*, 1706. [\[CrossRef\]](#)

31. Dawi, E.A.; Mustafa, E.; Padervand, M.; Ashames, A.; Hajiahmadi, S.; Saleem, L.; Baghernejad, M.; Nur, O.; Willander, M. Ag/AgCl decorated ionic liquid@tantalum pentoxide nanostructures: Fabrication, photocatalytic activity, and cytotoxicity effects against human brain tumor cells. *J. Inorg. Organomet. Polym.* **2023**. [[CrossRef](#)]
32. Gavazov, K.B.; Toncheva, G.K. Ion-association between some ditetrazolium cations and anions originated from 4-(2-thiazolylazo)resorcinol or 4-(2-pyridylazo)resorcinol. *Russ. J. Gen. Chem.* **2015**, *85*, 192–197. [[CrossRef](#)]
33. Alexandrov, A.; Simeonova, Z.; Kamburova, M. A relationship between association constants and the molecular mass of tetrazolium ion association complexes. *Bulg. Chem. Commun.* **1990**, *23*, 542–544.
34. Yuzhakov, V.I. Association of dye molecules and its spectroscopic manifestation. *Russ. Chem. Rev.* **1979**, *48*, 1076–1091. [[CrossRef](#)]
35. Konermann, L. Addressing a common misconception: Ammonium acetate as neutral pH “buffer” for native electrospray mass spectrometry. *J. Am. Soc. Mass Spectrom.* **2017**, *28*, 1827–1835. [[CrossRef](#)] [[PubMed](#)]
36. Zhiming, Z.; Dongsten, M.; Cunxiao, Y. Mobile equilibrium method for determining composition and stability constant of coordination compounds of the form  $M_mR_n$ . *J. Rare Earths* **1997**, *15*, 216–219.
37. Galan, T.R.; Ramirez, A.A.; Ceba, M.R. A new spectrophotometric method for differentiating mononuclear and polynuclear complexes and for determining their extraction constants. *Talanta* **1980**, *27*, 545–547. [[CrossRef](#)]
38. Job, P. Recherches sur la formation de complexes minéraux en solution, et sur leur stabilité. *Ann. Chim.* **1928**, *9*, 113–134.
39. Klausen, K.S.; Langmyhr, F.J. The use of the method of continuous variation for the classification of complexes with mole ratio 1:1. *Anal. Chim. Acta* **1963**, *28*, 335–340. [[CrossRef](#)]
40. Asmus, E. Eine neue Methode zur Ermittlung der Zusammensetzung schwacher Komplexe (A new method for the determination of composition of weak complexes). *Fresenius' J. Anal. Chem.* **1960**, *178*, 104–116. [[CrossRef](#)]
41. Bent, H.E.; French, C.L. The structure of ferric thiocyanate and its dissociation in aqueous solution. *J. Am. Chem. Soc.* **1941**, *63*, 568–572. [[CrossRef](#)]
42. Sayago, A.; Boccio, M.; Asuero, A.G. Continuous variation data: 1:1 or 2:2 weak complexes? *Int. J. Pharm.* **2005**, *295*, 29–34. [[CrossRef](#)]
43. Gavazov, K.B.; Toncheva, G.K.; Delchev, V.B. An extraction-chromogenic system for vanadium(IV,V) based on 2,3-dihydroxynaphthalene. *Open Chem.* **2016**, *14*, 197–205. [[CrossRef](#)]
44. Gavazov, K.B.; Delchev, V.B.; Mileva, K.T.; Stefanova, T.S.; Toncheva, G.K. A 2:2:2 complex of vanadium(V) with 4-(2-thiazolylazo)resorcinol and 2,3,5-triphenyl-2H-tetrazolium chloride. *Acta Chim. Slov.* **2016**, *63*, 392–398. [[CrossRef](#)] [[PubMed](#)]
45. Gavazov, K.B.; Stefanova, T.S. Liquid-liquid extraction-spectrophotometric investigations of three ternary complexes of vanadium. *Croat. Chem. Acta* **2014**, *87*, 233–240. [[CrossRef](#)]
46. Tōei, K. Ion-association reagents. A review. *Anal. Sci.* **1987**, *3*, 479–488. [[CrossRef](#)]
47. Racheva, P.V.; Milcheva, N.P.; Saravanska, A.D.; Gavazov, K.B. Extraction of gallium(III) with a new azo dye in the presence or absence of xylometazoline hydrochloride. *Croat. Chem. Acta* **2020**, *93*, 159–165. [[CrossRef](#)]
48. Racheva, P.V.; Milcheva, N.P.; Genç, F.; Gavazov, K.B. A centrifuge-less cloud point extraction-spectrophotometric determination of copper(II) using 6-hexyl-4-(2-thiazolylazo)resorcinol. *Spectrochim. Acta Mol. Biomol. Spectrosc.* **2021**, *262*, 120106. [[CrossRef](#)]
49. Likussar, W.; Boltz, D.F. Theory of continuous variations plots and a new method for spectrophotometric determination of extraction and formation constants. *Anal. Chem.* **1971**, *43*, 1265–1272. [[CrossRef](#)]
50. Holme, A.; Langmyhr, F.J. A modified and a new straight-line method for determining the composition of weak complexes of the form  $A_mB_n$ . *Anal. Chim. Acta* **1966**, *36*, 383–391. [[CrossRef](#)]
51. Harvey, A.E.; Manning, D.L. Spectrophotometric methods of establishing empirical formulas of colored complexes in solution. *J. Am. Chem. Soc.* **1950**, *72*, 4488–4493. [[CrossRef](#)]
52. Gjickaj, M.; Xie, T.; Brockner, W. Uncommon compounds in antimony pentachloride—Ionic liquid systems: Synthesis, crystal structure and vibrational spectra of the complexes  $[TPT][SbCl_6]$  and  $[Cl-EMIm][SbCl_6]$ . *Z. Anorg. Allg. Chem.* **2009**, *635*, 1036–1040. [[CrossRef](#)]
53. Stefanova-Bahchevanska, T.; Milcheva, N.; Zaruba, S.; Andruch, V.; Delchev, V.; Simitchiev, K.; Gavazov, K. A green cloud-point extraction-chromogenic system for vanadium determination. *J. Mol. Liq.* **2017**, *248*, 135–142. [[CrossRef](#)]
54. Mortada, W.I.; Zedan, H.E.; Khalifa, M.E. Spectrophotometric determination of trace vanadium in fresh fruit juice samples by ion pair-based surfactant-assisted microextraction procedure with solidification of floating organic drop. *Spectrochim. Acta Mol. Biomol. Spectrosc.* **2023**, *302*, 123107. [[CrossRef](#)] [[PubMed](#)]
55. Temel, N.K.; Kuş, B.; Gürkan, R. A new ion-pair ultrasound assisted-cloud point extraction approach for determination of trace V(V) and V(IV) in edible vegetal oils and vinegar by spectrophotometry. *Microchem. J.* **2019**, *150*, 104139. [[CrossRef](#)]
56. Peroković, V.P.; Ivšić, A.G.; Car, Ž.; Tomić, S. Synthesis of 3-hydroxy-1-(p-methoxyphenyl)-2-methylpyridine-4-one and spectrophotometric extraction studies on its complexation of vanadium(V). *Croat. Chem. Acta* **2014**, *87*, 103–109. [[CrossRef](#)]
57. Milcheva, N.P.; Genç, F.; Racheva, P.V.; Delchev, V.B.; Andruch, V.; Gavazov, K.B. An environmentally friendly cloud point extraction-spectrophotometric determination of trace vanadium using a novel reagent. *J. Mol. Liq.* **2021**, *334*, 116086. [[CrossRef](#)]
58. Agnihotri, R.; Agnihotri, N.; Kumar, V.; Kamal, R. Synthesis and application of 3-hydroxy-2-[3-(4-methoxyphenyl)-1-phenyl-4-pyrazolyl]-4-oxo-4h-1-benzopyran for extractive spectrophotometric determination of vanadium (V). *Der Chem. Sin.* **2017**, *8*, 158–165.
59. Gavazov, K.B.; Lekova, V.D.; Dimitrov, A.N.; Patronov, G.I. The solvent extraction and spectrophotometric determination of vanadium(V) with 4-(2-thiazolylazo)-resorcinol and tetrazolium salts. *Cent. Eur. J. Chem.* **2007**, *5*, 257–270. [[CrossRef](#)]

60. Khazal, H.; Mohammed, H.J.; Khazal, F. Spectrophotometric determination of trace amount of Vanadium in rice and flour using 1-[(4-antipyl azo)] 2-Naphthol as new chromogenic spectrophotometry. *J. Phys. Conf. Ser.* **2020**, *1660*, 012024. [[CrossRef](#)]
61. Pasha, C.; Sunil, K.; Stancheva, K. Crystal violet—A new reagent used for the spectrophotometric determination of vanadium. *Oxid. Commun.* **2022**, *45*, 503–513.
62. Gavazov, K.B.; Racheva, P.V.; Milcheva, N.P.; Divarova, V.V.; Kiradzhyska, D.D.; Genç, F.; Saravanska, A.D. Use of a hydrophobic azo dye for the centrifuge-less cloud point extraction–spectrophotometric determination of cobalt. *Molecules* **2022**, *27*, 4725. [[CrossRef](#)]
63. Frisch, M.J.; Trucks, G.W.; Schlegel, H.B.; Scuseria, G.E.; Robb, M.A.; Cheeseman, J.R.; Scalmani, G.; Barone, V.; Petersson, G.A.; Nakatsuji, H.; et al. *Gaussian 16*; Gaussian, Inc.: Wallingford, CT, USA, 2016.
64. ChemCraft. Available online: <http://www.chemcraftprog.com> (accessed on 13 September 2023).

**Disclaimer/Publisher’s Note:** The statements, opinions and data contained in all publications are solely those of the individual author(s) and contributor(s) and not of MDPI and/or the editor(s). MDPI and/or the editor(s) disclaim responsibility for any injury to people or property resulting from any ideas, methods, instructions or products referred to in the content.